NEUROSCIENCE

A shift in the mechanisms controlling hippocampal engram formation during brain maturation

Adam I. Ramsaran[1,2], Ying Wang[1,3], Ali Golbabaei[1,4], Stepan Aleshin[5], Mitchell L. de Snoo[1,4], Bi-ru Amy Yeung[1,3], Asim J. Rashid[1], Ankit Awasthi[1], Jocelyn Lau[1,3], Lina M. Tran[1,3,6], Sangyoon Y. Ko[1,3], Andrin Abegg[1,7]†, Lana Chunan Duan[1,4], Cory McKenzie[1,2], Julia Gallucci[1]‡, Moriam Ahmed[1], Rahul Kaushik[5,8], Alexander Dityatev[5,8,9], Sheena A. Josselyn[1,2,3,4,10], Paul W. Frankland[1,2,3,4,11]*

The ability to form precise, episodic memories develops with age, with young children only able to form gist-like memories that lack precision. The cellular and molecular events in the developing hippocampus that underlie the emergence of precise, episodic-like memory are unclear. In mice, the absence of a competitive neuronal engram allocation process in the immature hippocampus precluded the formation of sparse engrams and precise memories until the fourth postnatal week, when inhibitory circuits in the hippocampus mature. This age-dependent shift in precision of episodic-like memories involved the functional maturation of parvalbumin-expressing interneurons in subfield CA1 through assembly of extracellular perineuronal nets, which is necessary and sufficient for the onset of competitive neuronal allocation, sparse engram formation, and memory precision.

The episodic memory system is absent or immature at birth and develops during childhood. Accordingly, early event memories are imprecise or gist-like until ~5 to 8 years of age, when mnemonic precision increases (1–5). Hippocampal maturation is thought to underlie the emergence of precise episodic memories in humans and episodic-like memories in nonhuman animals (5–8), but the specific processes regulating memory precision during hippocampal development are unknown.

Age-dependent increases in engram sparsity track changes in the precision of hippocampus-dependent memories

The binding of events to their surrounding spatial context is a core feature of episodic and episodic-like memory that may be studied in animals using spatial or contextual learning tasks (9). To assess when this ability emerges during mouse development, we trained mice of different ages in contextual fear conditioning and tested their memory 24 hours later in either the same (context A) or a distinct (context B) testing apparatus (Fig. 1, A and B). Younger mice [postnatal day 16 (P16) to P20] expressed imprecise contextual fear memories, freezing at equivalent levels in the training context A and the novel context B. By contrast, older mice (≥P24) expressed context-specific memories, freezing more in context A than in context B (Fig. 1C). This shift in memory precision parallels similar shifts in rats (10), was independent of the animals' sex or weaning status, and did not depend on prior experience with contexts, potential age-dependent differences in learning rate, or ability to perceptually discriminate the contexts (fig. S1, A to S). Memory imprecision in juvenile mice scaled with the similarity between the training and testing contexts (fig. S1, T and U). Shifts in memory precision also occurred between P20 and P24 in a related aversive contextual learning task (inhibitory avoidance; fig. S1, V to X) and an appetitively motivated spatial foraging task (Fig. 1, D to F, and fig. S2, A to H).

Although contextual fear memories depend on the hippocampus in adult rodents (11), it is possible that this type of learning is supported by extrahippocampal structures in juvenile mice (12). This is consistent with proposals that the hippocampus does not support early event memories in children but instead "comes online" during childhood to allow the emergence of episodic memory (12, 13). We tested the hippocampal dependency of contextual fear memories in juvenile and adult mice by microinjecting adeno-associated viruses (AAVs) encoding inhibitory opsins into the dorsal CA1 of the hippocampus (fig. S3, A and B). CA1 may support both precise and imprecise memories across development (14, 15). Optogenetic silencing of CA1 pyramidal neurons impaired precise memory recall in P60 mice (11) (fig. C and D). In P20 mice, silencing CA1 neurons reduced freezing in both the A and B contexts, indicating that CA1 supports imprecise contextual memories at this developmental stage.

Although these results indicate that the immature hippocampus supports early memories, age-dependent differences in memory precision suggest that these memories may be encoded differently in the hippocampi of juvenile versus adult mice. In adults, context memories are encoded by sparse ensembles of neurons, known as engrams, in the hippocampus (16, 17). Given the imprecision of juvenile memories, we wondered whether CA1 engrams supporting contextual memories in juvenile mice lack sparsity. To identify putative engram neurons, we examined the expression of the activity-regulated immediate-early gene (IEG) c-Fos in the dorsal CA1 of P20, P24, and P60 mice after contextual fear conditioning (Fig. 1G). Training induced Fos expression in ~20% of CA1 neurons in P24 and P60 mice (18–20). By contrast, training induced c-Fos expression in ~40% of CA1 neurons in P20 mice, suggesting that engrams are more densely encoded in juvenile mice (Fig. 1H). Moreover, a similarly high proportion of c-Fos$^+$ CA1 neurons was observed in juvenile mice after testing (fig. S4, A to C) and in P20 "home cage" mice (fig. S4, D to H), consistent with observations that IEG expression is transiently elevated in the hippocampus of experimentally naïve rodents during the third postnatal week as the activity-dependent assembly of hippocampal neural circuitry nears completion (21–23).

CA1 engram sparsity controls memory precision

To test whether there is a causal relationship between engram size and memory precision, we investigated whether artificially shrinking engrams in juvenile mice would promote adult-like memory precision. We expressed the inhibitory designer receptor exclusively activated by designer drugs (DREADD) hM4Di in a subset of CA1 neurons and injected the DREADD ligand C21 before training to inhibit infected neurons and prevent their inclusion in the engram (Fig. 2A and fig. S5A). C21 treatment reduced engram size (training-induced c-Fos expression; Fig. 2, B and C), and these juvenile mice precociously exhibited adult-like memory precision (freezing more in context A than in context B) (Fig. 2, D and E, and fig. S5, B and C).

Conversely, we investigated whether artificially expanding the engram in adult mice would induce juvenile-like memory imprecision. We expressed the excitatory DREADD construct hM3Dq in pyramidal layer neurons (Fig. 2F and fig. S5D) and injected C21 before training to increase the activity of hM3D-infected neurons. C21 treatment increased engram size (training-induced c-Fos expression;

[1]Program in Neurosciences and Mental Health, The Hospital for Sick Children, Toronto, Ontario, Canada. [2]Department of Psychology, University of Toronto, Toronto, Ontario, Canada. [3]Department of Physiology, University of Toronto, Toronto, Ontario, Canada. [4]Institute of Medical Science, University of Toronto, Toronto, Canada. [5]Molecular Neuroplasticity, German Center for Neurodegenerative Diseases, Magdeburg, Germany. [6]Vector Institute, Toronto, Ontario, Canada. [7]Department of Biology, ETH Zürich, Zürich, Switzerland. [8]Center for Behavioral Brain Sciences, Magdeburg, Germany. [9]Medical Faculty, Otto von Guericke University, Magdeburg, Germany. [10]Brain, Mind, & Consciousness Program, Canadian Institute for Advanced Research, Toronto, Ontario, Canada. [11]Child & Brain Development Program, Canadian Institute for Advanced Research, Toronto, Ontario, Canada.
*Corresponding author. Email: paul.frankland@sickkids.ca
†Present addresses: Institute of Pharmacology and Toxicology, University of Zürich, Zürich, Switzerland, and Switzerland Neuroscience Center, University of Zürich, Zürich, Switzerland. ‡Present addresses: Campbell Family Mental Health Research Institute, Centre for Addiction and Mental Health, Toronto, Ontario, Canada, and Institute of Medical Science, University of Toronto, Toronto, Ontario, Canada.
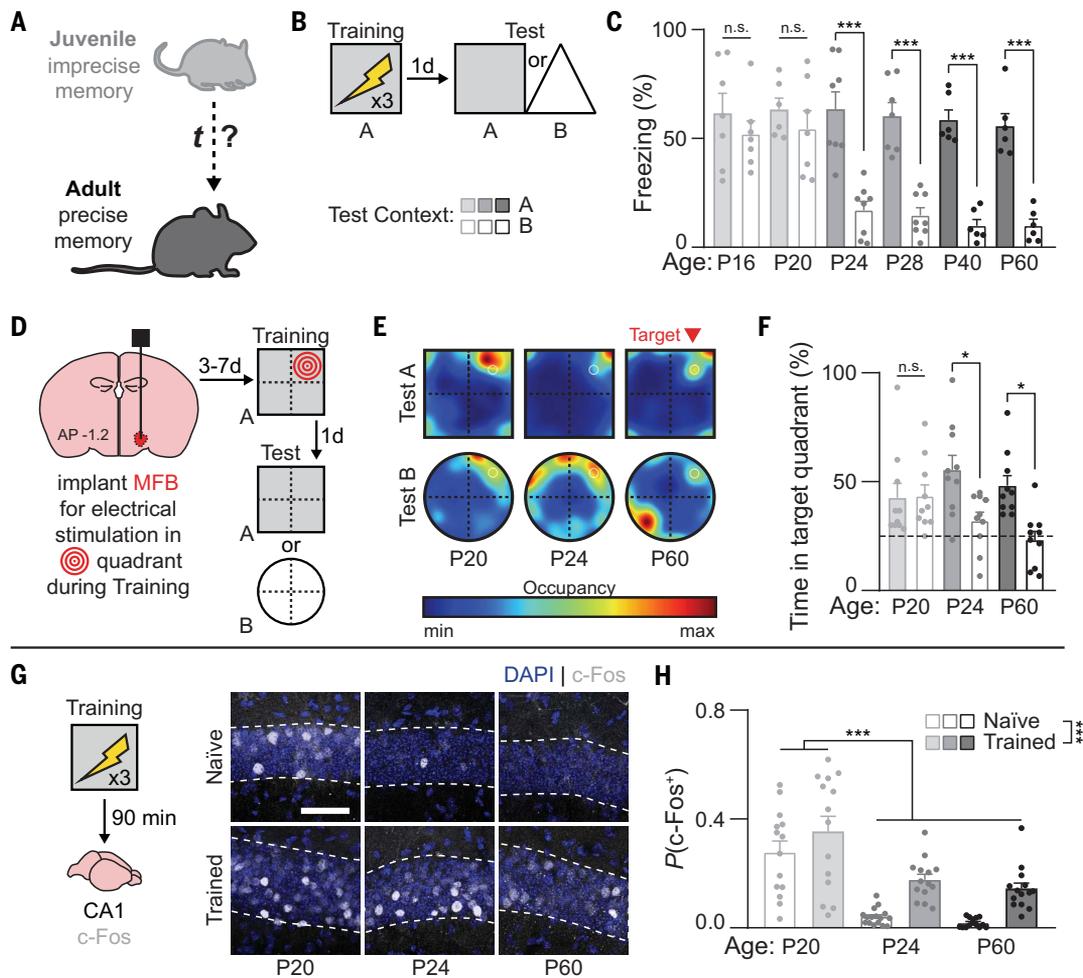
Fig. 1. Memory precision and sparse engrams develop in the dorsal CA1 during the fourth postnatal week. (**A**) The development of memory precision was assessed in mice. (**B**) Schematic of contextual fear conditioning protocol. (**C**) Juvenile mice (P16 to P20) formed imprecise contextual fear memories, whereas older (>P24) mice formed precise memories [analysis of variance (ANOVA), age × test context interaction: $F_{1,70} = 4.91$, $P < 0.001$]. (**D**) Schematic of spatial foraging task. (**E**) Heatmaps depicting the average search pattern of P20, P24, and P60 mice during the test session. (**F**) Juvenile mice (P20) formed imprecise spatial memories, whereas older (>P24) mice formed precise memories (ANOVA, age × test context interaction: $F_{2,54} = 3.65$, $P < 0.05$). (**G**) c-Fos expression in dorsal CA1 90 min after contextual fear conditioning. Images show c-Fos expression in a segment of the dorsal CA1 pyramidal layer. (**H**) Approximately twice as many CA1 pyramidal layer cells expressed c-Fos after conditioning (or in home cage) in P20 mice compared with conditioned P24 and P60 mice (ANOVA, main effect of age: $F_{2,80} = 34.81$, $P < 10^{-6}$; main effect of experience: $F_{1,80} = 20.50$, $P < 0.0001$). Data points are individual mice with mean ± SEM. Scale bar, 50 µm. *$P < 0.05$; ***$P < 0.001$.

Fig. 2, G and H), and these adult mice exhibited juvenile-like memory imprecision (equal freezing in contexts A and B) (Fig. 2, I and J, and fig. S5, E and F). Thus, the delayed onset of adult-like memory functions by hyperactivity within developing memory circuits may be a core feature of ontogeny across animal species (*24*).

Mature neuronal allocation develops during the fourth postnatal week in CA1

Such differences in engram sparsity between young and old mice suggest that the mechanisms of memory formation differ across development. In adult animals, eligible neurons are allocated to a sparse engram based on relative neuronal excitability or activity at the time of memory formation. To maintain en-

gram sparsity, not only are neurons with relatively higher excitability included in the engram, but neurons with relatively lower excitability are excluded from the engram through lateral inhibition (*25*). We probed how neuronal allocation changes across development. We injected a replication-defective herpes simplex virus (HSV) into dorsal CA1 to infect a sparse random population of neurons with both a blue light (BL)–sensitive excitatory opsin, ChR2, and red light (RL)–sensitive inhibitory opsin, eNpHR3.0 (HSV-NpACY; Fig. 3, A and B, and fig. S6A). This approach allowed us to bidirectionally modulate the activity of the same population of infected neurons with different wavelengths of light (*26*). We briefly excited NpACY^{+} neurons with BL immediately before conditioning to bias their allocation into the en-

gram. Control mice were treated similarly but received no BL. After training, c-Fos was preferentially expressed in NpACY^{+} neurons in P20, P24, and P60 mice in the BL[+] (allocated) but not BL[−] (control, nonallocated) groups (fig. S6, B to E), suggesting that optogenetically mediated allocation was effective regardless of mouse age.

In a second cohort of mice, we repeated the same allocation procedure and then determined whether infected neurons were necessary for subsequent memory expression by using RL to silence NpACY[+]-expressing neurons during a memory test. Silencing NpACY^{+} neurons impaired fear recall in P24 and P60 mice in the allocated group, but not in the control, nonallocated group (Fig. 3, C and D), indicating that the CA1 engram was localized to the

sparse NpACY+ population of neurons. By contrast, silencing a similar number of NpACY+ neurons did not impair fear memory recall in P20 mice. This suggests that information is more broadly distributed in densely encoded engrams in juvenile mice, such that silencing only a fraction of these neurons is not sufficient to disrupt memory recall. Consistent with this interpretation, a greater proportion of the dense juvenile engram was localized to NpACY− neurons (fig. S6F).

In juvenile mice, chemogenetic shrinking of the engram promoted adult-like neuronal allocation. Silencing allocated NpACY+ neurons impaired fear recall in the juvenile C21 group (Fig. 3, E to G), indicating that artificially shrinking the CA1 engram in P20 mice localized the memory to the sparse NpACY+ population of neurons. In adult mice, chemogenetic expansion of the engram induced juvenile-like neuronal allocation. Silencing allocated NpACY+ neurons no longer impaired fear memory recall in the adult C21 group (Fig. 3, H to J), consistent with the idea that information was not localized to the sparse population of NpACY+ neurons, but rather was more broadly distributed within the artificially expanded engram.

Maturation of parvalbumin-mediated inhibition is necessary for mature neuronal allocation and memory precision in CA1

The denser engrams in P20 mice raised the possibility that the second component of the mature neuronal allocation process, the exclusion of less-active or inactive neurons from engrams by interneurons, is not yet fully developed in juvenile mice. In the lateral amygdala, parvalbumin-expressing (PV+) basket cells provide strong somatic inhibition onto excitatory neurons at the time of memory formation to exclude less excitable neurons from the engram (26, 27). CA1 PV+ interneurons are born embryonically in the medial ganglionic eminence, resulting in adult-like levels of these cells by the third postnatal week in mice (6, 28) (Fig. 4, A and B). Despite their early birthdate, morphological and functional development of CA1 PV+ interneurons continues into the fourth postnatal week in mice (29, 30). Therefore, in P20 mice, developing PV+ interneurons in the CA1 may provide only weak lateral inhibition, precluding the formation of sparse engrams at the time of memory encoding. Adult-like levels of PV+ neurites and Syt2+ puncta (labeling PV+ interneuron presynaptic terminals; fig. S7A) emerged in the CA1 pyramidal layer at P24 (Fig. 4, C and D). Moreover, contextual fear conditioning increased the selectivity of perisomatic PV staining surrounding c-Fos− (compared with c-Fos+) pyramidal layer cells at P24 and P60, but not at P20, consistent with the idea that experience-dependent lateral inhibition does not occur
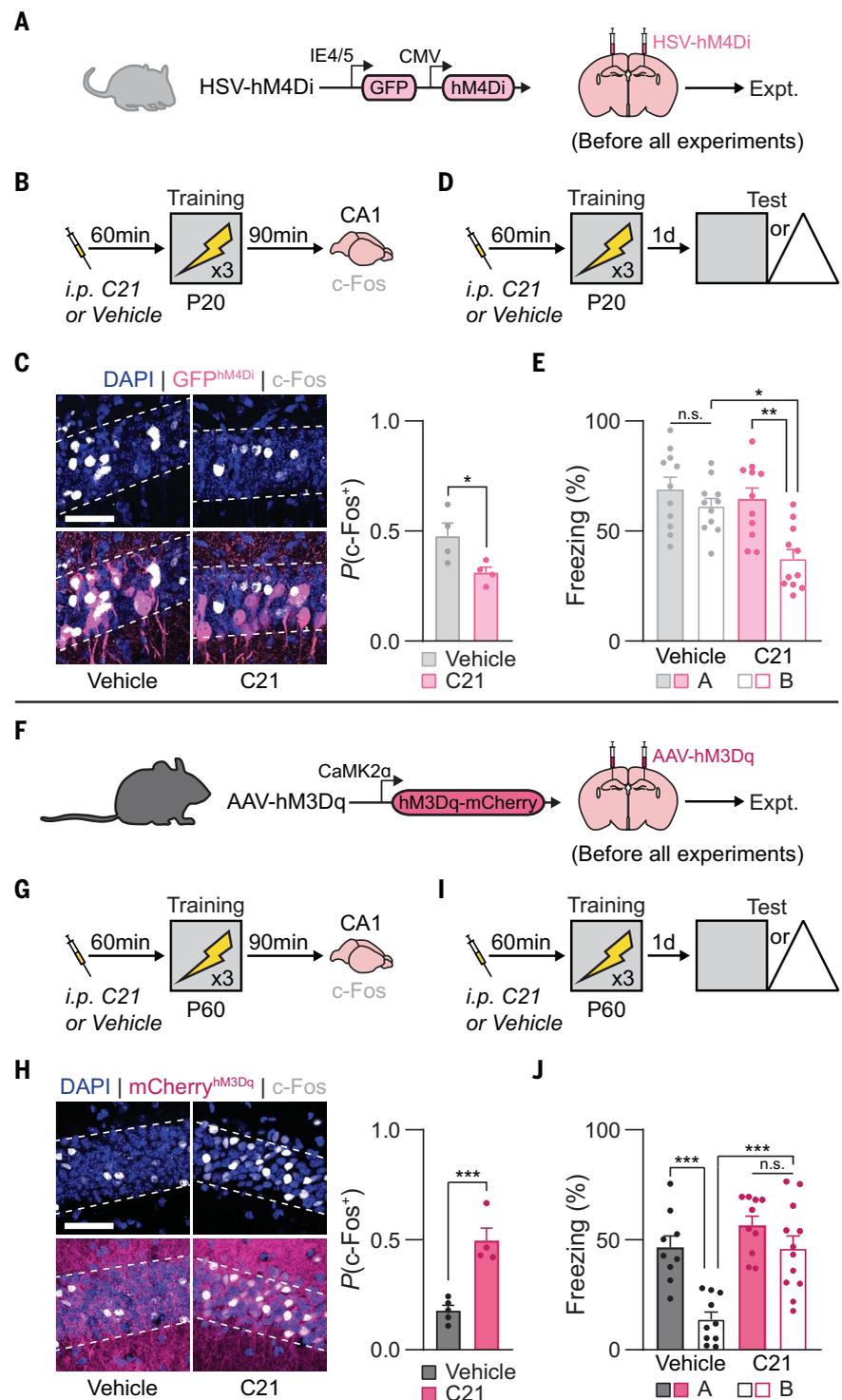
Fig. 2. Engram sparsity in the dorsal CA1 controls memory precision in juvenile and adult mice. (**A**) Engram size in dorsal CA1 of P20 mice was artificially decreased with HSV-hM4Di. (**B** and **C**) C21 was injected 1 hour before training (B) and reduced c-Fos expression in the juvenile CA1 (C) (unpaired t test: $t_6 = 2.57$, $P < 0.05$). (**D** and **E**) P20 mice administered C21 before training (D) formed precise contextual fear memories, and vehicle-treated P20 mice formed imprecise memories (E) (ANOVA, drug × test context interaction: $F_{1,26} = 4.48$, $P < 0.05$). (**F**) Engram size in dorsal CA1 of P60 mice was artificially increased with AAV-hM3Dq. (**G** and **H**) C21 was injected 1 hour before training (G) and increased c-Fos expression in the adult CA1 (H) (unpaired t test: $t_7 = 5.53$, $P < 0.001$). (**I** and **J**) P60 mice administered C21 before training (I) formed imprecise contextual fear memories, and vehicle-treated P60 mice formed precise memories (J) (ANOVA, drug × test context interaction: $F_{1,37} = 5.14$, $P < 0.05$). Data points are individual mice with mean ± SEM. Scale bars, 50 μm. *$P < 0.05$; **$P < 0.01$; ***$P < 0.001$.

before the fourth postnatal week (Fig. 4, E and F, and fig. S7, B to E).

Next, we expressed hM4Di in adult PV-Cre mice to inhibit PV$^+$ interneurons during memory formation (Fig. 4G and fig. S8, A and B).

Administering C21 before fear conditioning disinhibited local excitatory neurons, resulting in high levels of c-Fos in the CA1 after training (Fig. 4, H to J). Moreover, inhibiting CA1 PV$^+$ interneurons in adult mice promoted juvenile-

like allocation and memory imprecision (Fig. 4, K to O, and fig. S8, C and D). Reinstatement of these juvenile-like mnemonic phenotypes in adult PV-Cre mice required the presence of both hM4Di and C21 at the time of memory encoding (and not memory retrieval) (fig. S8, E to H). Thus, acute PV$^+$ interneuron inhibition at the time of memory formation was sufficient to phenocopy the allocation and memory specificity profile of juvenile mice while also maintaining the critical role of CA1 in encoding and retrieving these modified memories (fig. S8, I to L). These experiments identify maturation of CA1 inhibitory PV$^+$ circuitry as the key driver of memory development during the fourth postnatal week.

## Perineuronal nets regulate maturation of PV$^+$ interneurons in CA1

PV$^+$ interneurons play a pivotal role in the development of cortical sensory systems by closing transient windows of critical period plasticity (*31*). For example, PV$^+$ interneuron maturation closes the critical period for ocular dominance plasticity in the binocular primary visual cortex (V1b) in mice and rats (*32*). The maturation of perineuronal nets (PNNs), extracellular matrix (ECM) structures primarily ensheathing the soma and proximal dendrites of PV$^+$ interneurons, helps to drive PV$^+$ cell maturation in the cortex and hippocampus. By stabilizing excitatory synapses onto PV$^+$ interneurons and inhibitory synapses originating from PV$^+$ interneurons, mature PNNs increase PV$^+$ interneuron–mediated inhibition (*33–35*). Because PNN formation in V1b is necessary for the emergence of adult-like visual acuity, we reasoned that PNN formation in the hippocampus may similarly regulate the development of adult-like mnemonic specificity.

Mature PNNs represent a form of dense ECM composed of polymer chains of hyaluronan (HA), chondroitin sulfate proteoglycans (CSPGs) of the lectican family, tenascin-R, and link proteins (*36, 37*). To establish a detailed developmental profile of PNNs in the hippocampus, we visualized *Wisteria floribunda* agglutinin (WFA), CSPG brevican (BCAN), and hyaluronan and proteoglycan link protein 1 (HAPLN1) in situ. WFA$^+$ PNNs were found throughout the adult hippocampus (fig. S9, A to C). Hippocampal PNNs primarily surrounded PV$^+$ interneurons (except for fasciola cinereum and CA2 PNNs) (fig. S9, D to I) and developed postnatally. In CA1, adult-like levels of PNNs surrounding PV$^+$ interneurons were achieved by P24 in both male and female mice (Fig. 5, A to D, and fig. S10, A to P). CA1 PNN density was not altered by contextual fear conditioning (fig. S10, Q and R), suggesting that only microscale PNN alterations are induced by memory formation (*38*). In contrast to CA1, PV$^+$ interneuron–associated PNNs reached adult levels before P16 in the dorsal dentate
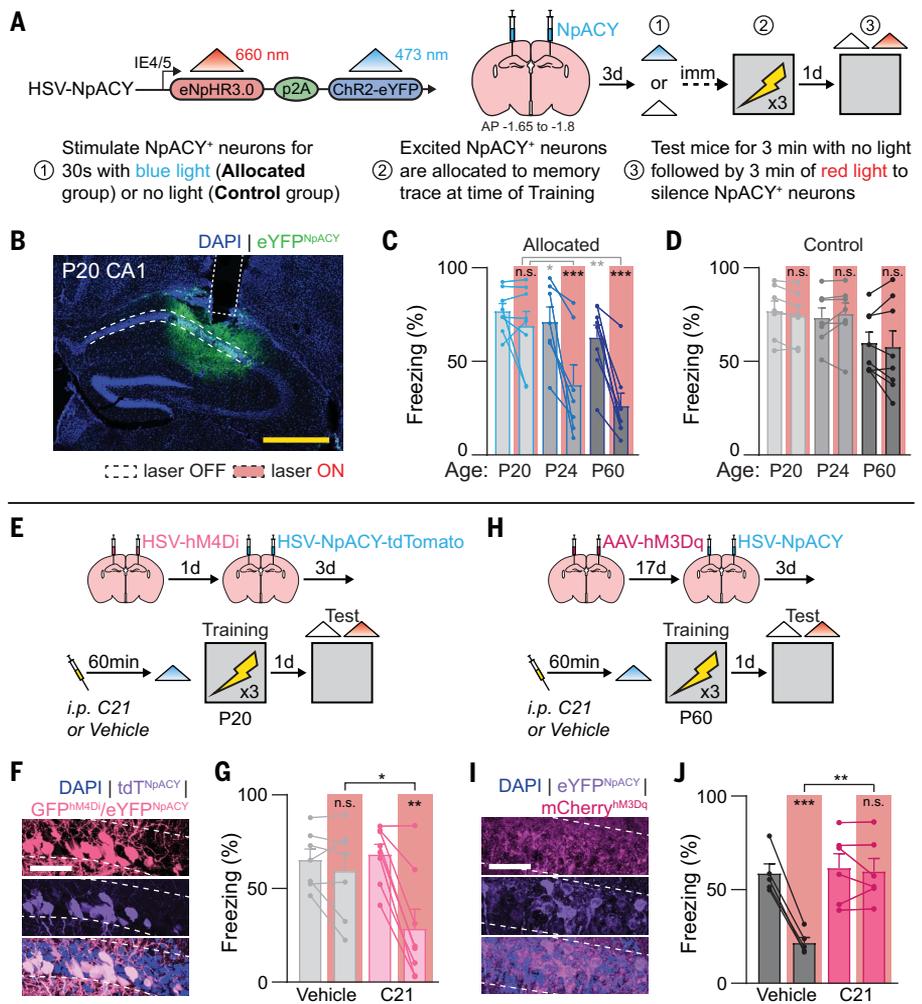
Fig. 3. Immature neuronal allocation mechanisms in the dorsal CA1 preclude localization of memories to sparse engrams during early development. (**A**) Schematic of the "allocate-and-silence" contextual fear conditioning protocol. HSV-NpACY was used to optogenetically excite (ChR2) and inhibit (NpHR3.0) the same neurons. (**B**) HSV-NpACY expression in dorsal CA1 of a P20 mouse. (**C**) Silencing a sparse group of NpACY$^+$ neurons previously allocated to the contextual fear memory engram impaired freezing during the test in P24 and P60 mice, but not P20 mice [repeated-measures (RM)–ANOVA, age × light interaction: $F_{2,20} = 4.96$, $P < 0.05$]. (**D**) Silencing a sparse group of random NpACY$^+$ neurons not allocated to the engram did not impair freezing during the test in any mice (RM-ANOVA, $P > 0.05$). (**E**) HSV-hM4Di and HSV-NpACY were both expressed in dorsal CA1 before contextual fear conditioning. C21 was administered 1 hour before training to promote sparse engram formation, and HSV-NpACY was used to allocate a sparse group of neurons to the engram at the time of training and to silence the same neurons during the test. (**F**) Expression of NpACY and hM4Di in the dorsal CA1 of a P20 mouse. (**G**) Silencing a sparse group of NpACY$^+$ neurons previously allocated to the contextual fear memory engram impaired freezing during the test in P20 mice that received C21 to shrink their engrams (RM-ANOVA, drug × light interaction: $F_{1,13} = 14.25$, $P < 0.01$). (**H**) AAV-hM3Dq and HSV-NpACY were both expressed in dorsal CA1 before contextual fear conditioning. C21 was administered 1 hour before training to promote dense engram formation, and HSV-NpACY was used to allocate a sparse group of neurons to the engram at the time of training and to silence the same neurons during the test. (**I**) Expression of NpACY and hM3Dq in the dorsal CA1 of a P60 mouse. (**J**) Silencing a sparse group of NpACY$^+$ neurons previously allocated to the contextual fear memory engram did not impair freezing during the test in P60 mice that received C21 to expand their engrams (RM-ANOVA, drug × light interaction: $F_{1,9} = 63.22$, $P < 0.0001$). Data points are individual mice with mean ± SEM. Scale bars: white, 50 μm; yellow, 500 μm. *$P < 0.05$; **$P < 0.01$; ***$P < 0.001$.
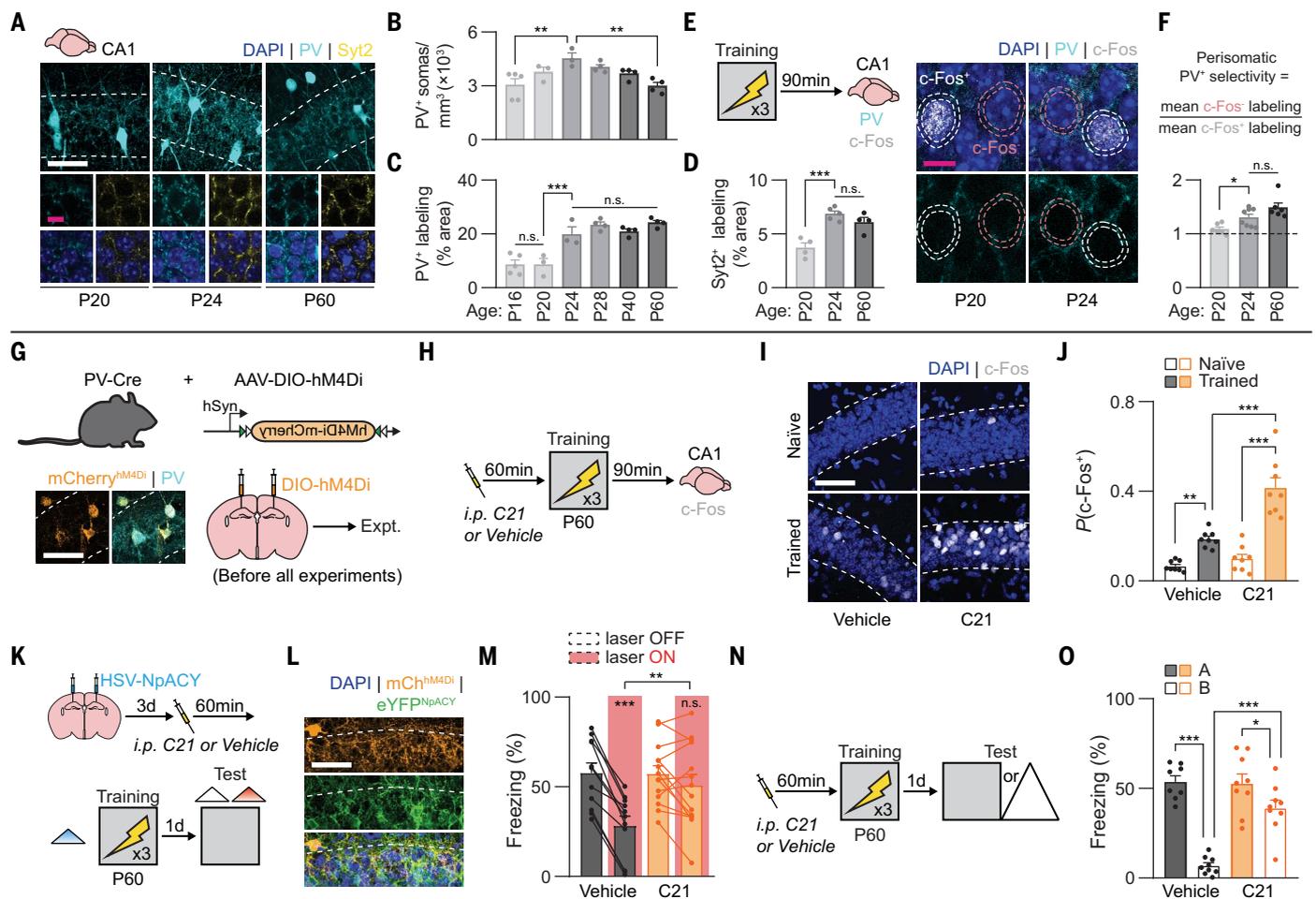
Fig. 4. Mature dorsal CA1 PV+ interneuron function is required for competitive neuronal allocation, sparse engram formation, and memory precision. (**A**) PV+ interneurons, PV+ neurites, and Syt2+ terminals in dorsal CA1 across development. (**B**) The number of PV+ interneurons peaks transiently at P24 (B) (ANOVA, effect of age: $F_{5,17} = 5.02$, $P < 0.01$). (**C** and **D**) The density of PV+ neurites (C) (ANOVA, effect of age: $F_{5,17} = 21.78$, $P < 10^{-5}$) and Syt2+ synaptic terminals (D) (ANOVA, effect of age: $F_{2,10} = 18.01$, $P < 0.001$) in the pyramidal layer reach adult-like levels by P24. (**E**) c-Fos and PV expression were examined in dorsal CA1 90 min after contextual fear conditioning. Localization of PV+ neurites around c-Fos− and c-Fos+ pyramidal layer cells is shown. PV+ labeling was quantified in a 3-μm ring surrounding the nuclei. (**F**) The selectivity of PV+ neurites around c-Fos− compared with c-Fos+ cells after training reached adult-like levels by P24 (ANOVA, effect of age: $F_{2,17} = 9.04$, $P < 0.01$). (**G**) PV+ interneurons were inhibited by expressing AAV-DIO-hM4Di in the dorsal CA1 of adult PV-Cre mice. (**H**) c-Fos expression in dorsal CA1 was examined 90 min after contextual fear conditioning. C21 was administered 1 hour before training to inhibit PV+ interneurons. (**I**) c-Fos expression in the dorsal CA1 pyramidal layer. (**J**) Inhibiting PV+ interneurons before training resulted in a twofold increase in c-Fos expression after training (ANOVA, drug × experience interaction: $F_{1,28} = 13.82$, $P < 0.001$). (**K**) Schematic of the contextual fear conditioning protocol. C21 was administered 1 hour before training to inhibit PV+ interneurons, and HSV-NpACY was used to excite (ChR2) and inhibit (NpHR3.0) the same neurons. (**L**) Expression of NpACY and hM4Di in the dorsal CA1 of a P60 mouse. (**M**) Silencing a sparse group of NpACY+ neurons previously allocated to the contextual fear memory engram did not impair freezing during the test in P60 mice that received C21 to inhibit their PV+ interneurons (RM-ANOVA, drug × light interaction: $F_{1,23} = 21.12$, $P < 0.001$). (**N**) Schematic of the contextual fear conditioning protocol. (**O**) P60 mice administered C21 to inhibit PV+ interneurons formed imprecise contextual fear memories, and vehicle-treated mice formed precise memories (ANOVA, drug × test context interaction: $F_{1,31} = 16.56$, $P < 0.001$). Data points are individual mice with mean ± SEM. Scale bars: magenta, 10 μm; white, 50 μm. *$P < 0.05$; **$P < 0.01$; ***$P < 0.001$.

gyrus and CA3 (fig. S11, A to K), consistent with the stepwise maturation of hippocampal trisynaptic circuitry (*21*).

HAPLN1 plays a key role in cross-linking and stabilizing CSPG-hyaluronan interactions, and *Hapln1* transcription corresponds with mature PNN formation in the cortex (*39*). To promote or interfere with PNN integrity, we designed viral vectors to overexpress wild-type full-length HAPLN1 (AAV-Hapln1) or mutant dominant-negative ΔHAPLN1 (AAV-ΔHapln1)

proteins tagged with cysteine-free green flourescent protein (cfGFP) or cfGFP only (AAV-cfGFP) (Fig. 5E). In contrast to full HAPLN1, ΔHAPLN1 did not promote binding of HA to lecticans (*40*), as we showed here for the first time (fig. S12, A to L). Expression of the constructs did not affect total endogenous expression of lecticans in the dorsal hippocampus of adult mice (fig. S13, A to L). However, AAV-ΔHapln1 expression destabilized CA1 PNNs in P60 mice and consequently reduced the den-

sity of PV+ neurites in the CA1 pyramidal layer (Fig. 5, F to J). By contrast, AAV-Hapln1 expression accelerated the maturation of CA1 PNNs and PV+ neurites in P20 mice (Fig. 5, K to O).

**PNN maturation regulates the emergence of neuronal allocation and memory precision in CA1**

First, we tested whether destabilizing CA1 PNNs in adult mice with AAV-ΔHapln1 would phenocopy the formation of a dense engrams and
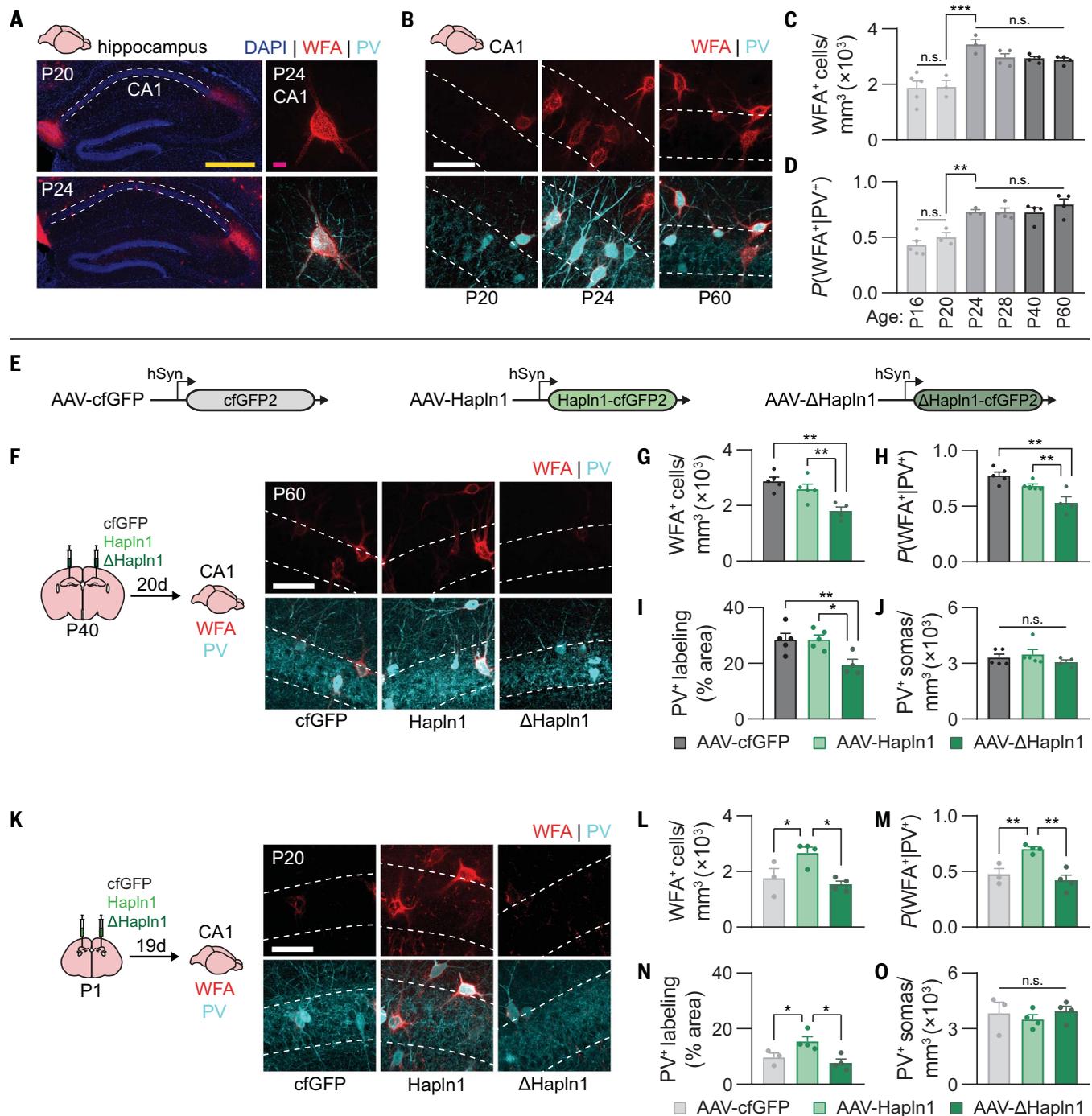
Fig. 5. Maturation of dorsal CA1 PNNs and PV⁺ interneurons requires HAPLN1.
(**A**) WFA⁺ PNNs in the hippocampus of a P20 and P24 mouse. High-magnification image of a WFA⁺ PNN on P24 surrounding the soma and proximal dendrites of a PV⁺ interneuron is shown. (**B**) WFA⁺ PNNs surrounding PV⁺ interneurons in dorsal CA1 across development. (**C** and **D**) The density of WFA⁺ PNNs in dorsal CA1 (ANOVA, effect of age: $F_{5,17} = 11.88$, $P < 0.0001$) surrounding PV⁺ interneurons (ANOVA, effect of age: $F_{5,17} = 13.51$, $P < 0.0001$) reached adult-like levels by P24. (**E**) To bidirectionally manipulate PNN integrity in vivo, we used AAV-Hapln1, AAV-ΔHapln1, and AAV-cfGFP to overexpress wild-type mouse HAPLN1 or a mutated dominant-negative ΔHAPLN1 or cfGFP as a negative control, respectively. (**F**) Mice were microinjected with AAVs, and P60 brains were stained for WFA⁺ PNNs and PV⁺ interneurons in the dorsal CA1. (**G** to **J**) Expression of AAV-ΔHapln1 in P60 CA1 decreased the number of WFA⁺ PNNs (G) (ANOVA, effect of virus:

$F_{2,11} = 10.88$, $P < 0.01$) surrounding PV⁺ interneurons (H (ANOVA, effect of virus: $F_{2,11} = 12.52$, $P < 0.01$), and density of PV⁺ neurites in the pyramidal layer (I) (ANOVA, effect of virus: $F_{2,11} = 6.88$, $P < 0.05$), without affecting the number of PV⁺ interneurons (J) (ANOVA, no effect of virus: $F_{2,11} = 0.89$, $P = 0.43$). (**K**) Mice were microinjected with AAVs, and P20 brains were stained for WFA⁺ PNNs and PV⁺ interneurons in the dorsal CA1. (**L** to **O**) Expression of AAV-Hapln1 in P20 CA1 increased the number of WFA⁺ PNNs (L) (ANOVA, effect of virus: $F_{2,8} = 8.02$, $P < 0.05$) surrounding PV⁺ interneurons (M) (ANOVA, effect of virus: $F_{2,8} = 14.43$, $P < 0.01$) and density of PV⁺ neurites in the pyramidal layer (N) (ANOVA, effect of virus: $F_{2,8} = 7.47$, $P < 0.05$) without affecting the number of PV⁺ interneurons (O) (ANOVA, no effect of virus: $F_{2,8} = 0.42$, $P = 0.66$). Data points are individual mice with mean ± SEM. Scale bars: magenta, 10 μm; white, 50 μm; yellow, 500 μm. *$P < 0.05$; **$P < 0.01$; ***$P < 0.001$.
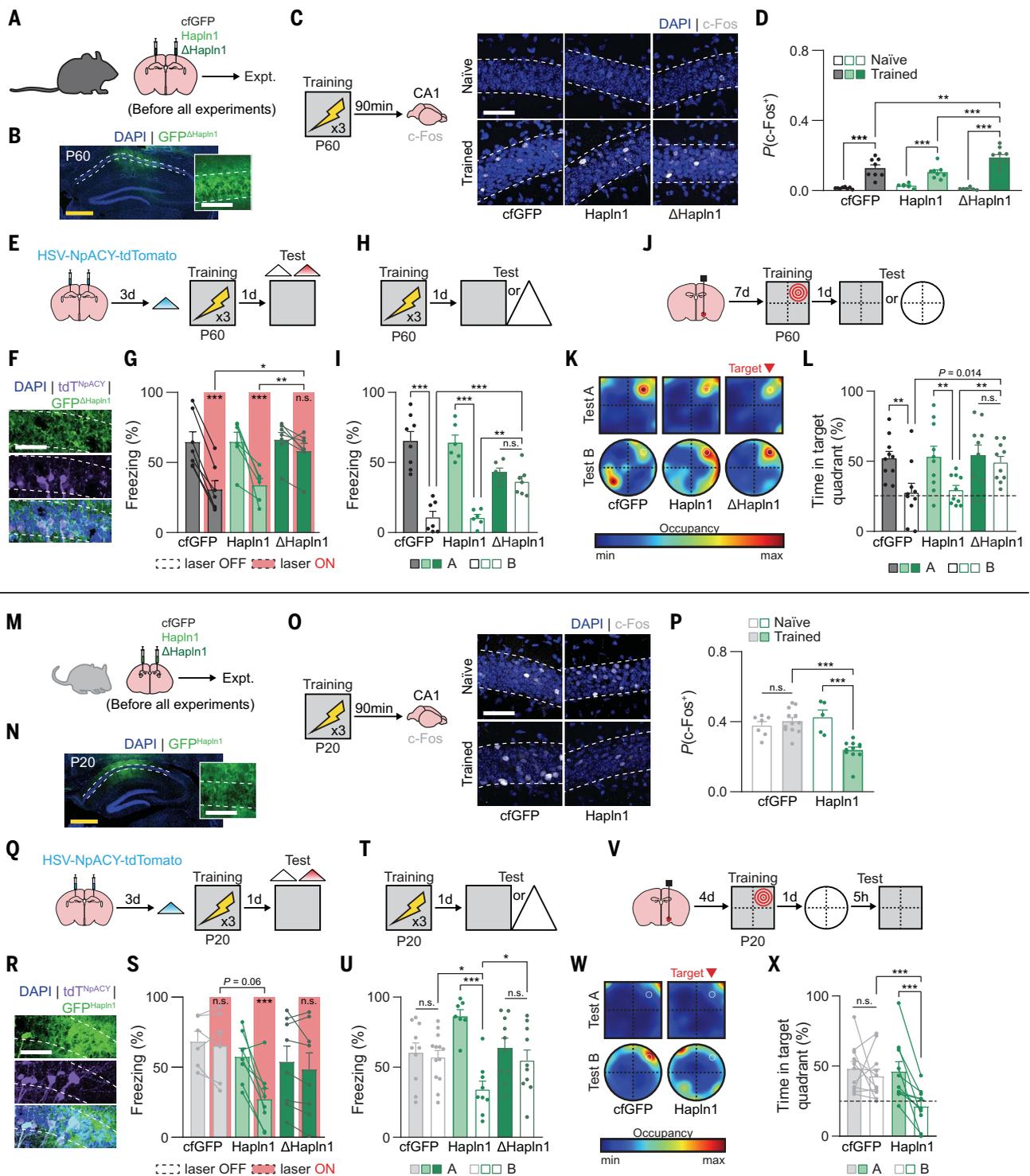
Fig. 6. Maturation of dorsal CA1 PNNs is required for competitive neuronal allocation, sparse engram formation, and memory precision. (**A**) PNNs were manipulated in the adult dorsal CA1 by microinjecting AAVs before each experiment. (**B**) AAV-ΔHapln1 expression in the P60 dorsal CA1. (**C**) c-Fos expression in dorsal CA1 was examined 90 min after contextual fear conditioning. (**D**) Expression of AAV-ΔHapln1 in P60 dorsal CA1 before training resulted in a twofold increase in c-Fos expression after training (ANOVA, virus × experience interaction: $F_{2,40} = 6.89$, $P < 0.01$). (**E**) Schematic of the contextual fear conditioning protocol. HSV-NpACY was used to optogenetically excite (ChR2) and inhibit (NpHR3.0) the same neurons. (**F**) Expression of NpACY and

AAV-ΔHapln1 in dorsal CA1 of P60 mouse. (**G**) Silencing a sparse group of NpACY+ neurons previously allocated to the contextual fear memory engram did not impair freezing during the test in P60 mice expressing AAV-ΔHapln1 in dorsal CA1 (RM-ANOVA, virus × light interaction: $F_{2,17} = 9.58$, $P < 0.01$). (**H**) Schematic of the contextual fear conditioning protocol. (**I**) P60 mice expressing AAV-ΔHapln1 in dorsal CA1 formed imprecise contextual fear memories, and P60 mice expressing AAV-cfGFP or AAV-Hapln1 formed precise memories (ANOVA, virus × test context interaction: $F_{2,34} = 16.40$, $P < 0.0001$). (**J**) Schematic of the spatial foraging task. (**K**) Heatmaps depicting example search patterns during the test. (**L**) P60 mice expressing AAV-ΔHapln1 in

dorsal CA1 formed imprecise spatial memories, and P60 mice expressing AAV-cfGFP or AAV-Hapln1 formed precise memories (unpaired t tests with Bonferroni correction, $\alpha = 0.01$, AAV-cfGFP context A versus context B: $t_{18} = 2.99$, $P < 0.01$; AAV-Hapln1 context A versus context B: $t_{18} = 2.90$, $P < 0.01$; AAV-ΔHapln1 context A versus context B: $t_{18} = 0.59$, $P = 0.56$; AAV-cfGFP context B versus AAV-ΔHapln1 context B: $t_{18} = 2.70$, $P = 0.014$; AAV-Hapln1 context B versus AAV-ΔHapln1 context B: $t_{18} = 3.61$, $P < 0.01$). (**M**) PNNs were manipulated in the juvenile dorsal CA1 by microinjecting AAVs before each experiment. (**N**) AAV-Hapln1 expression in the P20 dorsal CA1. (**O**) c-Fos expression in dorsal CA1 was examined 90 min after contextual fear conditioning. (**P**) Expression of AAV-Hapln1 in P20 dorsal CA1 before training resulted in a decrease in c-Fos expression after training (ANOVA, virus × experience interaction: $F_{1,31} = 19.07$, $P < 0.001$). (**Q**) Schematic of the contextual fear conditioning protocol. HSV-NpACY was used to optogenetically excite (ChR2) and inhibit (NpHR3.0) the same neurons. (**R**) Expression of NpACY and AAV-Hapln1 in the dorsal CA1 of P20 mouse. (**S**) Silencing a sparse group of NpACY⁺ neurons previously allocated to the contextual fear memory engram impaired freezing during the test in P20 mice expressing AAV-Hapln1 in dorsal CA1 (RM-ANOVA, virus × light interaction: $F_{2,19} = 8.10$, $P < 0.01$). (**T**) Schematic of the contextual fear conditioning protocol. (**U**) P20 mice expressing AAV-Hapln1 in CA1 formed precise contextual fear memories, and P20 mice expressing AAV-cfGFP or AAV-ΔHapln1 formed imprecise memories (ANOVA, virus × test context interaction: $F_{2,53} = 7.83$, $P < 0.01$). (**V**) Schematic of the spatial foraging task. (**W**) Heatmaps depicting example search patterns during the test. (**X**) P20 mice expressing AAV-Hapln1 in dorsal CA1 formed precise spatial memories, and P20 mice expressing AAV-cfGFP formed imprecise memories (RM-ANOVA, virus × test context interaction: $F_{1,19} = 4.09$, $P = 0.05$). Data points are individual mice with mean ± SEM. Scale bars: white, 50 μm; yellow, 500 μm. *$P < 0.05$; **$P < 0.01$; ***$P < 0.001$.

memory imprecision typical of juvenile mice (Fig. 6, A and B). In CA1 of adult mice overexpressing ΔHAPLN1 (but not cfGFP or wild-type HAPLN1), training-induced PV-mediated lateral inhibition was precluded (fig. S14, A to C) and dense c-Fos⁺ engrams formed (Fig. 6, C and D), resulting in intact memory when sparse populations of artificially allocated NpACY⁺ neurons were silenced during testing (Fig. 6, E to G). CA1 PNN destabilization in separate groups of adult mice produced imprecise contextual fear memory (Fig. 6, H and I, and fig. S15, A and B) and appetitive spatial memory (Fig. 6, J to L, and fig. S16, A and B). The effects of ΔHAPLN1 in adult mice were specific to episodic-like memory formation. Destabilization of CA1 PNNs with AAV-ΔHapln1 did not decrease precision for auditory fear memories or increase anxiety-like behavior or locomotion in an open field (fig. S15, C to G). Changes in contextual memory precision were largely restricted to manipulation of PNNs in CA1 (and not cortex) (fig. S15, H to K), which we also observed using the enzyme ChABC (35) to transiently digest PNNs (figs. S15, L to O, and S17, A to R).

Finally, we tested whether accelerating PNN maturation with AAV-Hapln1 was sufficient to produce adult-like memory phenotypes of sparse engram formation and precise contextual memories (Fig. 6, M and N). We observed adult-like neuronal allocation in CA1 of juvenile mice overexpressing wild-type HAPLN1, evidenced by the early onset of PV-mediated lateral inhibition (fig. S14, D to F) and sparse c-Fos⁺ engram formation (Fig. 6, O and P). Consistent with sparse engram formation, silencing sparse populations of artificially allocated NpACY⁺ neurons impaired memory recall in juveniles expressing AAV-Hapln1, but not AAV-cfGFP or AAV-ΔHapln1 (Fig. 6, Q to S), and these mice formed precise fear memories (Fig. 6, T and U, and fig. S15, P and Q) and reward memories (Fig. 6, V to X, and fig. S16, D and E). Similarly, direct infusion of recombinant brain-derived neurotrophic factor, a treatment that accelerates maturation of neural circuits (32), into CA1 on P17 also resulted in the precocial maturation of PNNs, PV⁺ interneurons, and memory precision in juvenile mice (fig. S18, A to I).

Discussion

The specific neurobiological mechanisms regulating age-dependent increases in the precision of episodic and episodic-like memory have long remained elusive (5, 7, 8). We found that the developing CA1 is actively engaged in early memory formation despite the immaturity of some memory formation mechanisms. Our findings identify engram sparsity as a key determinant of memory precision. Specifically, we identified maturation of a competitive neuronal allocation process, supported by developing PV⁺ interneurons, as a prerequisite for encoding precise, episodic-like memories in sparse engrams. These findings support the recent proposal that the hippocampus transitions through distinct stages of functional development, with the stepwise emergence of CA1 phenomena important for memory consolidation (41, 42). These processes disproportionately affect engram neurons (43, 44), providing potential mechanisms for post-encoding stabilization of sparse engrams during the fourth postnatal week and onward.

We discovered that maturation of PV⁺ inhibitory circuitry required for the onset of adult-like neuronal allocation and episodic-like memory precision in CA1 are dependent on the extracellular matrix PNNs. In mammalian and avian brains, the accumulation of PNNs around PV⁺ interneurons in defined cortical regions shifts local excitatory-inhibitory balance, dampens critical period plasticity, and controls the development of corresponding sensory processes or behaviors (31, 35, 37, 39). Our data suggest that maturation of the hippocampal memory system is regulated by the same cellular and molecular mechanisms as cortical sensory systems. They also indicate that memory formation changes the relative levels of perisomatic inhibition of engram neurons through PNN-dependent mechanisms, likely mediated in part by the PNN glycoprotein tenascin-R (45). Therefore, ECM-dependent maturation of inhibitory neural circuits may be a brainwide mechanism for not only sensory development, but also cognitive and emotional development (34, 46–48).

Why are there multiple stages of functional maturation in the development of the hippocampal memory system? One possibility is that hippocampal development involves progression of the episodic memory system from an "incomplete" (child-like) to a "complete" (adult-like) state. An alternative possibility is that the mnemonic functions of children are perfectly adapted for their stage of development (49). At the cognitive level, the encoding of schemas and other forms of broad or imprecise semantic knowledge during early life may be favored over encoding specific episodes, given that young children have comparatively few life experiences from which to draw and typically are not without parents or alloparents (with fully fledged episodic memory systems) for the first years of life (50). The immature hippocampus may have evolved to fulfill this purpose, exploiting the protracted development of inhibition and co-opting the same activity-dependent mechanisms required for structural and functional development of hippocampal circuitry (21–23) for early memory formation and storage in dense memory engrams.

REFERENCES AND NOTES

1. C. T. Ngo, Y. Lin, N. S. Newcombe, I. R. Olson, *J. Exp. Psychol. Gen.* **148**, 1463–1479 (2019).
2. L. Picard, S. Cousin, B. Guillery-Girard, F. Eustache, P. Piolino, *Child Dev.* **83**, 1037–1050 (2012).
3. H. Yim, A. F. Osth, V. M. Sloutsky, S. J. Dennis, *Psychol. Sci.* **33**, 1154–1171 (2022).
4. L. Rollins, E. B. Cloude, *Learn. Mem.* **25**, 294–297 (2018).
5. J. Bachevalier, F. Vargha-Khadem, *Curr. Opin. Neurobiol.* **15**, 168–174 (2005).
6. R. Cossart, R. Khazipov, *Physiol. Rev.* **102**, 343–378 (2022).
7. A. Keresztes, C. T. Ngo, U. Lindenberger, M. Werkle-Bergner, N. S. Newcombe, *Trends Cogn. Sci.* **22**, 676–686 (2018).
8. A. I. Ramsaran, M. L. Schlichting, P. W. Frankland, *Dev. Cogn. Neurosci.* **36**, 100591 (2019).
9. T. A. Allen, N. J. Fortin, *Proc. Natl. Acad. Sci. U.S.A.* **110** (Suppl 2), 10379–10386 (2013).
10. M. J. Anderson, D. C. Riccio, *Learn. Behav.* **33**, 444–453 (2005).
11. I. Goshen *et al.*, *Cell* **147**, 678–689 (2011).
12. L. Nadel, S. Zola-Morgan, "Infantile amnesia," in *Infant Memory*, M. Moscovitch, Ed. (Springer, 1984), vol. 9, pp. 145–172.
13. J. Bachevalier, M. Mishkin, *Behav. Neurosci.* **98**, 770–778 (1984).
14. C. T. Ellis *et al.*, *Curr. Biol.* **31**, 3358–3364.e4 (2021).

15. A. C. Schapiro, N. B. Turk-Browne, M. M. Botvinick, K. A. Norman, *Philos. Trans. R. Soc. Lond. B Biol. Sci.* **372**, 20160049 (2017).
16. S. A. Josselyn, S. Köhler, P. W. Frankland, *Nat. Rev. Neurosci.* **16**, 521–534 (2015).
17. J. T. Wixted *et al.*, *Proc. Natl. Acad. Sci. U.S.A.* **111**, 9621–9626 (2014).
18. K. Z. Tanaka *et al.*, *Science* **361**, 392–397 (2018).
19. K. K. Tayler, K. Z. Tanaka, L. G. Reijmers, B. J. Wiltgen, *Curr. Biol.* **23**, 99–106 (2013).
20. D. J. Cai *et al.*, *Nature* **534**, 115–118 (2016).
21. F. Donato, R. I. Jacobsen, M.-B. Moser, E. I. Moser, *Science* **355**, eaai8178 (2017).
22. A. Travaglia, R. Bisaz, E. Cruz, C. M. Alberini, *Neurobiol. Learn. Mem.* **135**, 125–138 (2016).
23. X. Gao *et al.*, *Proc. Natl. Acad. Sci. U.S.A.* **115**, 12531–12536 (2018).
24. S. G. Leinwand, K. Scott, *Neuron* **109**, 1836–1847.e5 (2021).
25. S. A. Josselyn, P. W. Frankland, *Annu. Rev. Neurosci.* **41**, 389–413 (2018).
26. A. J. Rashid *et al.*, *Science* **353**, 383–387 (2016).
27. D. J. Morrison *et al.*, *Neurobiol. Learn. Mem.* **135**, 91–99 (2016).
28. F. Donato, A. Chowdhury, M. Lahr, P. Caroni, *Neuron* **85**, 770–786 (2015).
29. D. Doischer *et al.*, *J. Neurosci.* **28**, 12956–12968 (2008).
30. L. Que, D. Lukacsovich, W. Luo, C. Földy, *Nat. Commun.* **12**, 108 (2021).
31. T. K. Hensch, *Nat. Rev. Neurosci.* **6**, 877–888 (2005).
32. Z. J. Huang *et al.*, *Cell* **98**, 739–755 (1999).
33. E. Dzyubenko *et al.*, *Cell. Mol. Life Sci.* **78**, 5647–5663 (2021).
34. E. Favuzzi *et al.*, *Neuron* **95**, 639–655.e10 (2017).
35. T. Pizzorusso *et al.*, *Science* **298**, 1248–1251 (2002).
36. J. W. Fawcett, T. Oohashi, T. Pizzorusso, *Nat. Rev. Neurosci.* **20**, 451–465 (2019).
37. O. Senkov, P. Andjus, L. Radenovic, E. Soriano, A. Dityatev, *Prog. Brain Res.* **214**, 53–80 (2014).
38. V. Nagy *et al.*, *J. Neurosci.* **26**, 1923–1934 (2006).
39. D. Carulli *et al.*, *Brain* **133**, 2331–2347 (2010).
40. K. Matsumoto *et al.*, *J. Biol. Chem.* **278**, 41205–41212 (2003).
41. U. Farooq, G. Dragoi, *Science* **363**, 168–173 (2019).
42. A. Figurov, L. D. Pozzo-Miller, P. Olafsson, T. Wang, B. Lu, *Nature* **381**, 706–709 (1996).
43. Y. Jeong *et al.*, *Nat. Commun.* **12**, 3915 (2021).
44. H. Norimoto *et al.*, *Science* **359**, 1524–1527 (2018).
45. A. K. Saghatelyan *et al.*, *Eur. J. Neurosci.* **12**, 3331–3342 (2000).
46. M. T. Birnie, T. Z. Baram, *Science* **376**, 1055–1056 (2022).
47. E. M. Nabel, H. Morishita, *Front. Psychiatry* **4**, 146 (2013).
48. N. Gogolla, P. Caroni, A. Lüthi, C. Herry, *Science* **325**, 1258–1261 (2009).
49. R. V. Kail, N. E. Spear, in *Comparative Perspectives on the Development of Memory*, R. V. Kail, N. E. Spear, Eds. (Psychology Press, 1984); pp. 325–358.
50. A. Gopnik, *Philos. Trans. R. Soc. Lond. B Biol. Sci.* **375**, 20190502 (2020).
51. A. Ramsaran *et al.*, Data for: A shift in the mechanisms controlling hippocampal engram formation during brain maturation, Dryad (2023).

ACKNOWLEDGMENTS

SUPPLEMENTARY MATERIALS

science.org/doi/10.1126/science.ade6530
Materials and Methods
Figs. S1 to S18
References (*52–70*)
MDAR Reproducibility Checklist

View/request a protocol for this paper from *Bio-protocol*.

A shift in the mechanisms controlling hippocampal engram formation during brain maturation

Adam I. Ramsaran, Ying Wang, Ali Golbabaei, Stepan Aleshin, Mitchell L. de Snoo, Bi-ru Amy Yeung, Asim J. Rashid, Ankit Awasthi, Jocelyn Lau, Lina M. Tran, Sangyoon Y. Ko, Andrin Abegg, Lana Chunan Duan, Cory McKenzie, Julia Gallucci, Moriam Ahmed, Rahul Kaushik, Alexander Dityatev, Sheena A. Josselyn, and Paul W. Frankland

Editor's summary

The hippocampal episodic memory system is not present at birth but develops during childhood. Ramsaran *et al.* examined hippocampal engrams in juvenile and adult mice and identified a cascade of events that underlie the emergence of episodic-like memory precision. The immature hippocampus forms dense engrams and imprecise memories. The ability to form sparse engrams does not emerge until the fourth postnatal week with the maturation of inhibitory circuits in the hippocampus. The maturation of perineuronal nets, extracellular matrix structures primarily ensheathing the soma and proximal dendrites of parvalbumin-containing interneurons, helps to drive inhibitory interneuron maturation in the cortex and hippocampus. —Peter Stern

View the article online
https://www.science.org/doi/10.1126/science.ade6530
Permissions
https://www.science.org/help/reprints-and-permissions

Use of this article is subject to the Terms of service